

A Dinuclear Ruthenium(II) Complex with the Dianion of 2,5-Dihydroxy-1,4-benzoquinone as Bridging Ligand. Redox, Spectroscopic, and Mixed-Valence Properties

Michael D. Ward

School of Chemistry, University of Bristol,
Cantock's Close, Bristol BS8 1TS, U.K.

Received July 13, 1995

Introduction

Dinuclear complexes containing polypyridyl–Ru(II) fragments have been of particular interest for the study of mixed valency because of their kinetic inertness in both the +2 and +3 oxidation states, generally reversible electrochemical behavior, and good π -donor capability which allows interaction with bridging ligand orbitals.¹ Many of the bridging ligands used in such binuclear complexes are also polypyridyl-based, and although significant metal–metal interactions can occur *via* metal–ligand $d(\pi)$ – π^* overlap, these may be limited by the considerable energy gap between the ruthenium $d(\pi)$ and ligand-based π^* levels.¹ Dioxolene-based ligands in contrast have orbitals of π symmetry which are much closer in energy to those of metal-based $d(\pi)$ orbitals, and recently much effort has been devoted to the study of the very rich electrochemical and spectroscopic properties of mononuclear ruthenium complexes with a variety of dioxolene ligands.² Since strong metal–metal interactions in binuclear complexes (resulting, for example, in class III mixed-valence behavior and large comproportionation constants for the mixed-valence state) are facilitated by electron delocalization from the metals toward the bridging ligand, binucleating bridging ligands based on dioxolenes are excellent candidates for use in the preparation of such complexes.³ We describe here the synthesis, electrochemical and spectroscopic properties of $[(\text{bipy})_2\text{Ru}]_2(\mu\text{-L})[\text{PF}_6]_2$ (**1**) where L^{2-} is the dianion of 2,5-dihydroxy-1,4-benzoquinone. This ligand presents an *O,O*-donor binding site to each metal ion in which one oxygen atom is formally quinonoidal and the other is anionic, so the binding site is similar to that presented by a semiquinone with the important exception that L^{2-} is diamagnetic. L^{2-} has been shown to be an effective mediator of electron-transfer in intramolecular redox reactions,⁴ as well as mediating electrochemical⁵ and magnetic exchange⁶ interactions in a variety of binuclear and polynuclear complexes.

Experimental Section

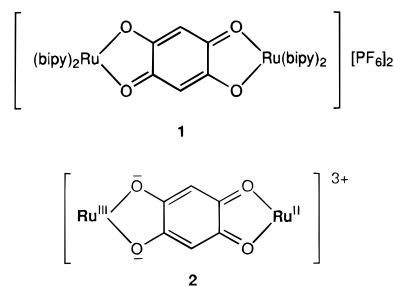
General Details. K_2L^7 and $[\text{Ru}(\text{bipy})_2\text{Cl}_2]\cdot 2\text{H}_2\text{O}^8$ were prepared according to the published methods. The apparatus used for standard spectroscopic and electrochemical measurements has been described

in detail elsewhere.⁹ The EPR spectra were recorded on a Bruker ESP-300E spectrometer; electrochemical generation of the reduced complex was performed by using an OTTL-type arrangement with a Pt-grid working electrode in a conventional EPR flat cell, modified by addition of a reservoir to accommodate the reference (SCE) and auxiliary (Pt wire) electrodes.

Preparation of $[(\text{bipy})_2\text{Ru}]_2(\mu\text{-L})[\text{PF}_6]_2$ (1**).** A mixture of K_2L (0.1 g, 0.46 mmol) and $[\text{Ru}(\text{bipy})_2\text{Cl}_2]\cdot 2\text{H}_2\text{O}$ (0.48 g, 0.92 mmol) in ethylene glycol (20 cm^3) was heated to 190 °C for 1 h under N_2 . After cooling, the complex was precipitated by addition of aqueous $\text{NH}_4\text{-PF}_6$, filtered off, washed with water, and dried. The crude complex could be purified either by recrystallization (MeCN/Et₂O) or chromatography on alumina (MeCN/toluene, 1:1). Anal. Calcd for $\text{C}_{46}\text{H}_{34}\text{F}_{12}\text{N}_8\text{O}_4\text{P}_2\text{Ru}_2$: C, 44.0; H, 2.7; N, 8.9. Found: C, 43.7; H, 2.7; N, 8.7. MS (FAB, 3-nitrobenzyl alcohol matrix): $m/z = 1111$ (100%, $\{1 - \text{PF}_6\}$), 966 (75%, $\{1 - 2\text{PF}_6\}$). ¹H NMR, CD_3CN , δ - (ppm): 5.95 (2 H, s), 7.18 (4 H, ddd, $J = 7.3, 5.7, 1.4$ Hz), 7.67 (8 H, m), 7.82 (4 H, td, $J = 7.8, 1.3$ Hz), 8.14 (4 H, td, $J = 7.9, 1.4$ Hz), 8.38 (4 H, d, $J = 7.9$ Hz), 8.50 (8 H, m). Yield: 60%.

Results and Discussion

Complex **1** is formed by reaction of K_2L with 2 equiv of $[\text{Ru}(\text{bipy})_2\text{Cl}_2]\cdot 2\text{H}_2\text{O}$ at high temperatures and is a purple-black solid with an intense inky purple color in solution. The FAB mass spectrum and elemental analysis confirmed its formulation, and the ¹H NMR spectrum shows the two protons of the bridging ligand as a singlet at 5.95 ppm with the expected intensity (2 H) relative to the eight bipyridyl proton resonances (4 H each).



The results of a molecular orbital calculation on the complex using the ZINDO method¹⁰ are presented in Figure 1, which shows the relative energies of the frontier orbitals. The HOMO contains substantial contributions from both the metals [Ru $d(xz)$ orbitals] and the bridging ligand; the density of the HOMO is 20% at each of the Ru atoms, with the remaining 60% being distributed over the bridging ligand. The LUMO in contrast is almost entirely composed of the bridging ligand π^* orbital (94%) with small contributions from the metal $d(xz)$ orbitals (3% each). The extent of mixing between the metals and the bridging ligand is less than that which occurs with simple dioxolenes such as the *o*-benzosemiquinone anion (sq), presumably due to the higher energy of the π^* level of L^{2-} arising from the double negative charge; although the π^* level of L^{2-} does lie below the bipy π^* levels, it is still substantially higher than the ruthenium $d(\pi)$ orbitals.

Cyclic and square-wave voltammetry (Figure 2) shows the presence of two reversible, one-electron oxidations at $E_{1/2} = +0.36$ and $+0.70$ V *vs* the ferrocene/ferrocenium couple (Fc/

- Ward, M. D. *Chem. Soc. Rev.* **1995**, 121 and references therein.
- (a) Auburn, P. R.; Dodsworth, E. S.; Haga, M.; Liu, W.; Nevin, W. A.; Lever, A. B. P. *Inorg. Chem.* **1991**, *30*, 3502. (b) Masui, H.; Lever, A. B. P.; Auburn, P. R. *Inorg. Chem.* **1991**, *30*, 2402 and references therein. (c) Haga, M.; Dodsworth, E. S.; Lever, A. B. P. *Inorg. Chem.* **1986**, *25*, 447.
- (a) Dei, A.; Gatteschi, D.; Pardi, L. *Inorg. Chem.* **1990**, *29*, 1442. (b) Joulié, L. F.; Schatz, E.; Ward, M. D.; Weber, F.; Yellowlees, L. J. *J. Chem. Soc., Dalton Trans.* **1994**, 799. (c) Sadler, G. G.; Gordon, N. R. *Inorg. Chim. Acta* **1991**, *180*, 271.
- Lu, K.; Earley, J. E. *Inorg. Chem.* **1993**, *32*, 189.
- Calvo, M. A.; Lanfredi, A. M. M.; Oro, L. A.; Pinillos, M. T.; Tejel, C.; Tiripicchio, A.; Ugozzoli, F. *Inorg. Chem.* **1993**, *32*, 1147.
- Fujii, C.; Mitsumi, M.; Kodera, M.; Motoda, K.; Ohba, M.; Matsumoto, N.; Okawa, H.; *Polyhedron* **1994**, *13*, 933 and references therein.
- Jones, R. G.; Shonle, H. A. *J. Am. Chem. Soc.* **1945**, *67*, 1034.
- Sullivan, B. P.; Salmon, D. J.; Meyer, T. J. *Inorg. Chem.* **1978**, *17*, 3334.

- Bardwell, D. A.; Barigelletti, F.; Cleary, R. L.; Flamigni, L.; Guardigli, M.; Jeffery, J. C.; Ward, M. D. *Inorg. Chem.* **1995**, *34*, 2438.
- The ZINDO calculations were performed on a CACHE workstation (CACHE Scientific, Beaverton, OR, USA, 1994) using the program supplied (written by M. C. Zerner) with the INDO/1 parameters. The molecule was first constructed using the Editor, and then energy-minimised using the Molecular Mechanics package with MM2 parameters. The energy-minimized structure was then used for the molecular orbital calculations.

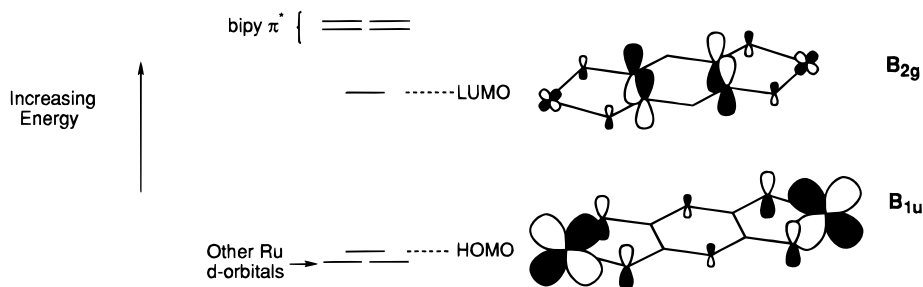


Figure 1. Frontier orbitals of **1**. The absolute energies are not given but the relative separations between orbitals are to scale. The symmetry labels for the orbitals assume D_{2h} local symmetry (i.e. the sense of coordination of the bipyridyl chelates is ignored). The x -axis is the Ru–Ru axis, and the z -axis is perpendicular to the plane of the bridging ligand.

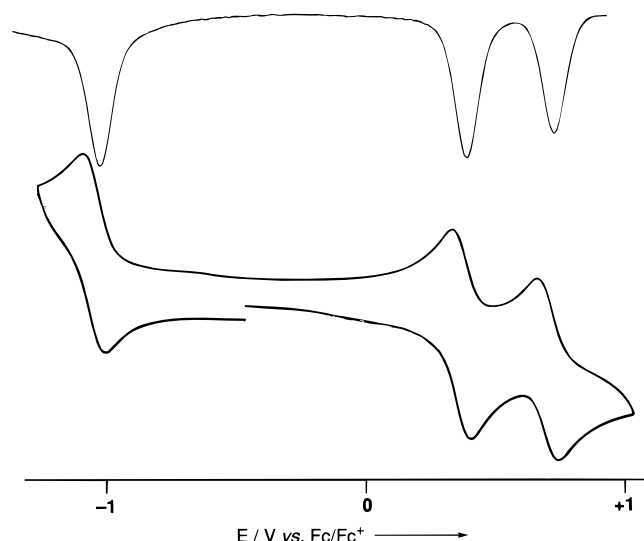


Figure 2. Osteryoung square-wave (upper trace) and cyclic (lower trace) voltammograms of **1** at a Pt-bead working electrode in MeCN containing 0.1 M $[\text{Bu}_4\text{N}][\text{PF}_6]$ as base electrolyte. The scan rate was 0.2 V s^{-1} .

Fc^+). By “reversible” is meant that the ratio of the cathodic and anodic peak currents is approximately unity at a variety of scan rates, and the peak-peak separations ΔE_p lie in the range 60–80 mV. These could be considered formally as metal-based Ru(II)/Ru(III) couples, although on the basis of the MO picture they have substantial ligand-based character. Their potentials are comparable to those of $[(\text{bipy})_2\text{Ru}]_2(\mu\text{-OMe})_2]^{2+}$ in which the array of donor atoms and charges about the Ru centers is similar to that of **1**.¹¹ The separation of 0.34 V between these couples corresponds to a comproportionation constant K_c of ca. 6×10^5 .

There is also a reversible one-electron wave at $E_{1/2} = -1.05 \text{ V vs Fc/Fc}^+$ which is on the predominantly ligand-centered LUMO. We investigated this by recording the EPR spectrum of the reduced species, generated either by controlled potential electrolysis in an EPR cell or by chemical reduction with cobaltocene in dry MeCN under N_2 . In each case a sharp signal was observed at $g = 2.063$ with a peak–peak separation of ca. 3 G (Figure 3); the spectrum of the chemically-reduced species is much broader than that of the electrochemically-reduced species, possibly due to being present in a higher concentration, but the essential parameters are the same. Shoulders on either side of the main peak are ascribable to weak hyperfine coupling to ruthenium, which has two isotopes with $I = 5/2$ (^{99}Ru and ^{101}Ru , combined abundance 29.8%): coupling to two equivalent Ru atoms would therefore give a singlet (49% of total intensity), a 1:1:1:1:1:1 sextet (42% of total intensity), and a 1:2:3:4:5:6:

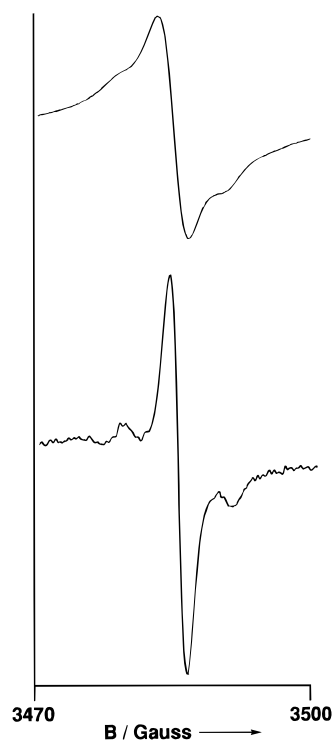


Figure 3. Solution EPR spectra in MeCN of the one-electron reduction product of **1**, prepared by chemical reduction with cobaltocene (upper trace) or electrochemically (lower trace).

5:4:3:2:1 undecet (9% of total intensity). The appearance of the spectra suggests that the two shoulders are the outer components of the sextet, with the outer components of the undecet being too weak to see. The hyperfine coupling A_{Ru} is therefore one-fifth of the separation between these components, i.e. 2.1 G. The narrow width of the signal is consistent with the expected predominantly ligand-centered organic radical species; however the deviation from the free-spin position and the weak coupling to ruthenium indicates a slight degree of delocalization of the electron onto the metals.¹²

Further ligand-based reductions occur at the extreme of the solvent window (beyond -2 V vs Fc/Fc^+), but the individual waves are obscured by sharp spikes from surface processes. These are likely to be bipy-based processes; a second reduction of the bridging ligand is also possible.

The electronic spectrum of **1** (Figure 4) contains transitions at 242, 293, 330, 506, and 721 nm in MeCN. The first two of these are typical ligand-centered (LC) $\pi \rightarrow \pi^*$ transitions, and the 506 nm transition we assign to a Ru(II) \rightarrow bipy(π^*) MLCT process.¹³ The most notable feature of the spectrum is the very

(11) Bardwell, D. A.; Jeffery, J. C.; Joulié, L.; Ward, M. D. *J. Chem. Soc., Dalton Trans.* **1993**, 2255.

(12) Connelly, N. G.; Manners, I.; Protheroe, J. R. C.; Whitely, M. W. *J. Chem. Soc., Dalton Trans.* **1984**, 2713.

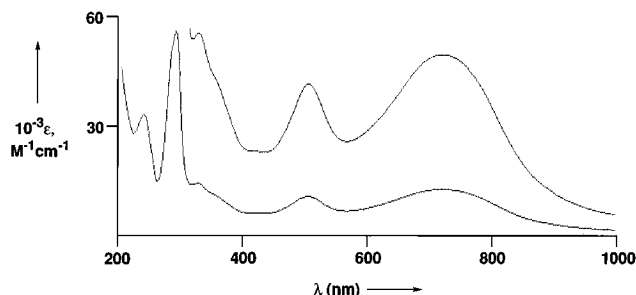


Figure 4. Electronic spectrum of **1** in MeCN (expansion is $\times 4$).

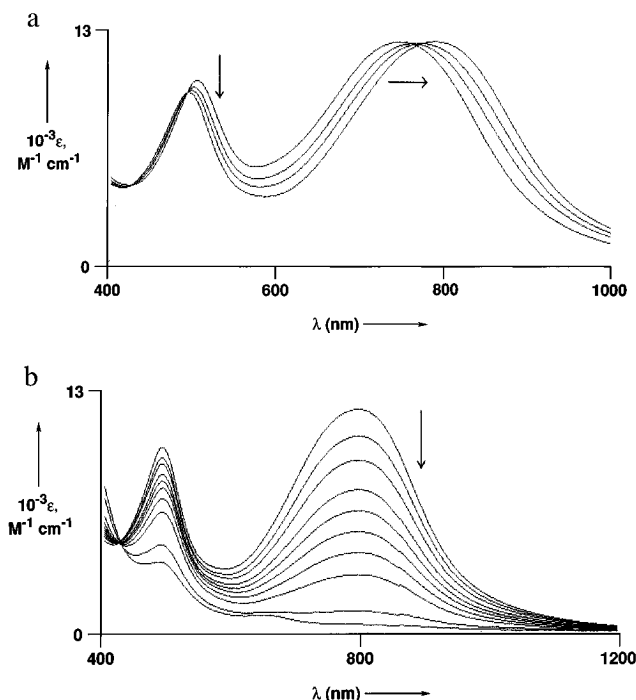


Figure 5. Successive electronic spectra of **1** recorded (a) during the $+2 \rightarrow +3$ oxidation and (b) during the $+3 \rightarrow +4$ oxidation, in dmf/water (3:1 v/v).

intense, broad band at 721 nm ($\epsilon = 12\,200\text{ M}^{-1}\text{ cm}^{-1}$) which is a transition from the HOMO (both metal- and ligand-based) to the LUMO (largely ligand-based), and therefore has both MLCT and LC character; for simplicity we will call this a Ru(II) \rightarrow L(π^*) transition even though this description is not wholly accurate. This transition is similar to Ru(II) \rightarrow semiquinone MLCT transitions with other dioxolene ligands,^{2c,3b} although it is at a rather high energy; in [Ru(bipy)₂(sq)]⁺ for example the Ru(II) \rightarrow (sq) MLCT transition is at 880 nm in MeCN due to the lower π^* level of the sq radical anion.^{2c} It is slightly solvatochromic, with λ_{max} taking the following values in different solvents: CH₂Cl₂, 720 nm; acetone and MeCN, 721 nm; MeOH, 728 nm; dmf and pyridine, 735 nm; dmsO, 743 nm; dmf/water (3:1, v/v), 745 nm; dmf/water (2:1), 751 nm (all values ± 2 nm). This is in accord with what would be expected for a transition which has some vectorial charge-transfer character.

The spectral region between 400 and 1800 nm was examined during a spectrophotometric titration in which **1** was successively oxidised from the dicationic state to the +3 and finally +4 states by addition of numerous small portions of the oxidant [Bu₄N][Br₃] (Figure 5). Due to the relatively low solubilities of the oxidized species it was necessary to use dmf/H₂O (3:1)

as solvent to prevent precipitation; unfortunately this limits the available spectral window to 1800 nm since at longer wavelengths there are multiple intense solvent absorptions. On oxidation of **1** by one electron to the +3 state the changes in the electronic spectrum are not dramatic: the Ru(II) \rightarrow bipy(π^*) transition is slightly blue-shifted from 506 to 493 nm with a slight drop in intensity, whereas the Ru(II) \rightarrow L(π^*) transition is red-shifted from 745 to 797 nm and remains at the same intensity. This suggests that the valences are localized and that these two Ru transitions in the mixed-valence state involve the remaining Ru(II) center; the Ru(II) \rightarrow L(π^*) band is red-shifted due to the increased positive charge distributed between the bridging ligand itself and the metal ion at the far end of the bridge. On further oxidation of the +3 state to the +4 state, both the Ru(II) \rightarrow L(π^*) and Ru(II) \rightarrow bipy(π^*) transitions disappeared, which is to be expected. A weak new transition at ca. 650 nm has appeared, which is likely to be a pyridyl \rightarrow Ru(III) LMCT.¹⁴

We found no evidence for the expected inter-valence charge transfer (IVCT) band in the spectrum of the +3 (mixed-valence) species within the spectral window available. There are two possible reasons for this. First, the mixed-valence state could be a relatively weakly interacting class II species, in which case the IVCT band would be at high energy and of low intensity: λ_{max} values of < 1000 nm and ϵ values of a few hundred are common.¹ Such a band would be obscured by the intense Ru(II) \rightarrow L(π^*) transition, which is very broad and has $\epsilon \approx 1800\text{ M}^{-1}\text{ cm}^{-1}$ at $\lambda = 1000$ nm. The second possibility is that the mixed-valence complex is class III, with an exceptionally low-energy IVCT band: for example the mixed-valence complex [(bipy)₂Ru]₂(μ -tetrox)]³⁺ has an IVCT band at $\lambda_{\text{max}} = 2080$ nm, the lowest energy known for such a transition.^{3a} Although this wavelength lies outside the spectral window we had available, a transition in this region would be very broad on a wavelength scale and a rise in the baseline at 1800 nm would certainly be apparent, which it was not. For an IVCT band to be at a sufficiently low energy for the baseline at 1800 nm to be flat is so far unprecedented for a ruthenium complex. The former explanation—that **1** has a class II mixed-valence state whose weak IVCT band is obscured—is much more likely, and is consistent with (i) the K_c value, which is rather lower than that of the Creutz–Taube ion ($K_c \approx 3 \times 10^6$, corresponding to a “borderline” class II/class III species); (ii) the spectroscopic evidence for a localized Ru(II) center in the mixed-valence state; and (iii) the possibility of charge redistribution in the bridging ligand which would stabilize a valence-localized state. The 2-fold degeneracy of the mixed-valence state (the odd electron could be associated with either metal) could be lifted by an unsymmetrical distortion involving a redistribution of electron density in the bridging ligand (structure **2**), such that the Ru(II) center is bound to a quinone-type binding site and the Ru(III) center is bound to a dianionic catechol-type binding site. In the absence of strong delocalization of electrons *via* Ru($d\pi$)–L(π^*) overlap this would be favored energetically,¹⁵ and is consistent with the observed valence-localized mixed-valence state.

Acknowledgment. Thanks are extended to Miss R. Bunn and Mr. F. Weber for assistance with the synthesis, to Dr. J. Maher for recording the EPR spectra, and to the CAChe Higher Education Support Program for provision of the CAChe workstation and software.

IC950877C

(13) Juris, A.; Balzani, V.; Barigelletti, F.; Campagna, S.; Belser, P.; von Zelewsky, A. *Coord. Chem. Rev.* **1988**, *84*, 85.

(14) Bryant, G. M.; Ferguson, J. E. *Aust. J. Chem.* **1971**, *24*, 275.

(15) Johnson, E. C.; Sullivan, B. P.; Salmon, D. J.; Adeyemi, S. A.; Meyer, T. J. *Inorg. Chem.* **1978**, *17*, 2211.